

Dynamic projecting IR zoom based systems

Benjamin E. Sturlesi

Sturlesi Computational Engineering, 84 Hanassi Ave., Haifa 34529, Israel,

Sami Mangoubi* and Emanuel Ben-David

CI Systems Ltd., Industrial Park 10551, Migdal Haemek, Israel

ABSTRACT

An IR target simulating projector system may sometimes require zooming lenses to simulate continuously the target's increasing size as a missile closes the range. In addition, special opto-mechanical layouts may sometimes be needed to allow cascaded action of two or more zooms to increase the zooming range, or to present to the missile simultaneously two or more spectral regions.

The zooms in these systems may differ in some important characteristics from the more conventional types: a) The maximum speed and acceleration of their moving parts, as required by the dynamics of the missile-target approach scenario, are to be limited by the performance of commercially available stages carrying those parts, and b) the motion control system must assure strict adherence to the "zoom function" (relative position of the zoom's moving parts) to avoid defocusing during the zooming phase.

In this paper we describe the implications of complying with these requirements on implementations actually designed and executed.

Keywords: Zooms, Infrared zooms, Dynamic zooms, Infrared dynamic simulation for missiles, Simulation of infrared scenes by zoom, Infrared dynamic zoom systems

1. INTRODUCTION

The incorporation of a dynamic zoom into a projecting system has been described in two previous papers^{1,2}, the main theme of which was to show that a realistic simulation can be achieved by optically combining different channels each providing an element of the dynamically evolving scene (target, background, or countermeasures). One or more of these channels could in principle generate its particular contribution by using a dynamic zoom to simulate continuously and in real-time the increasing size of an object as the missile closes the range. No details were provided in those papers as to the special characteristics demanded of a zoom used in such a dynamic fashion, to be a faithful reproduction of the approach scenario.

In our present paper we analyze the properties of the zoom function (the Effective Focal Length or EFL dependence on the lens-groups positions) and the relations that must exist between it and the pursuit function so as to make the simulation realistic and correct. An example is provided as an application of these new principles.

* Presently at the Armament Authority, Haifa, Israel

2. DYNAMIC ZOOM SYSTEMS

A Dynamic Zoom is hereby defined as a variable EFL lens system, changeable continuously in real-time mode. Dynamic zooms are, as a rule, incorporated into projecting simulators to project into a missile's optical head (UUT - Unit Under Test) the increasing size of a target as seen by the missile during its flight in a closing range approach or pursuit scenario. The movable lens groups of the zoom system are mounted on stages controlled by servos to effect a programmed real-time change of EFLs as demanded by that scenario. Speeds and accelerations applicable to the stages mounted with lenses are naturally mechanically or otherwise limited, and complying with these limitations for the envelope of envisaged pursuits produces new restricting boundaries to be observed in the optical design space. These new bounds may significantly reduce the freedom of choice of the designer for zooms destined to be dynamic with commonly available commercial stages. As a matter of fact most projecting dynamic zooms designed and developed by the authors are dynamically limited, in the sense just defined, inter alia by the minimum closing range and maximum final closing speeds of pursuit scenarios correctly simulated, as well as by the braking relief required to stop the stages safely at the hitting end.

The mathematical relations interconnecting the pursuit parameters of the missile-target approach to the zoom opto-mechanical characteristics are given hereunder. If "t" stands for the time independent variable, "r(t)" for the radial (scalar) missile-target range as a function of time, "f(t)" for the EFL of the variable zoom, "x(t)" for a movable stage position relative to any fixed marker on this zoom with "t(x)" its inverse, and "f(t(x))" the combined function giving the EFL dependence on that stage position, then for the simulator to project correctly a fixed size target transparency into the UUT's optics as a true simulation of a constant size real target moving at a radial velocity "dr/dt" relative to it, the EFL must change at a proportional rate, namely

$$df/dt = (f/r)dr/dt,$$

f/r being constant. The stage velocity then follows directly as

$$dx/dt = dx/df * df/dt = (f * dx/df) * (1/r * dr/dt), \quad (1)$$

r being supposed large enough to make negligible the target image shift from the lens infinite conjugate. Taking the second derivatives of (1)

$$d^2x/dt^2 = d/dt(f * dx/df) * (1/r * dr/dt) + (f * dx/df) * d/dt(1/r * dr/dt). \quad (2)$$

The first term on the right hand side of (2) becomes:

$$d/dt(f * dx/df) * (1/r * dr/dt) = d/df(f * dx/df) * df/dx * dx/dt * (1/r * dr/dt).$$

Replacing dx/dt with the explicit stage velocity (1) one obtains for this first term:

$$\begin{aligned} d/dt(f * dx/df) * (1/r * dr/dt) &= d/df(f * dx/df) * f * (1/r * dr/dt)^2 = \\ &= (f * dx/df + f^2 * d^2x/df^2) * (1/r * dr/dt)^2. \end{aligned} \quad (3)$$

Next, the second term on the right side of (2) then becomes:

$$(f * dx/df) * d/dt(1/r * dr/dt) = f * dx/df * (1/r * d^2r/dt^2 - (1/r * (dr/dt))^2). \quad (4)$$

On adding (3) and (4) and simplifying, the stage acceleration takes the form:

$$d^2x/dt^2 = (f^2 * d^2x/df^2) * (1/r * dr/dt)^2 + (f * dx/df) * (1/r * d^2r/dt^2) \quad (5)$$

Examining (1) and (5) it transpires that there exist two 'indicators':

a 'velocity indicator': $f * dx/df$,

and

an 'acceleration indicator': $f^2 * d^2x/df^2$,

that are characteristic of the zoom design and that depend solely on its optical behavior. Together, they may serve to combine the instantaneous missile-target radial approach velocity dr/dt and radial acceleration d^2r/dt^2 with the characteristics of the zoom's EFL function of stage position, to comply correctly with a specific pursuit scenario. The physical dimension of both indicators being [L], the units systematically chosen in this paper to represent them are millimeters.

Projecting zooms are in addition required to have an external, and usually far removed, (exit) pupil. The UUT entrance admission being the constraining stop of the entire optical layout, its real images throughout the system are real, fully illuminated pupils. No vignetting by lens boundaries is, as rule, permitted during the entire zooming range, to avoid infiltration of unwanted external radiation into the UUT. To the best knowledge of the authors, little or no information exists in the published professional literature as to the characteristics and designs of such zooms.

Fortunately, both velocity and acceleration indicators can be fully assessed from the 1st order behavior of a zooming system of lenses. At this first order stage, group spacing means air-separation between their appropriate principal planes. All higher order development then following, namely, beefing up the groups, achromatizing the combination and correcting or balancing the monochromatic aberrations does not affect these indicators.

3. A PRACTICAL EXAMPLE

The application of this mathematical analysis is shown for the case of a 10 degrees FOV, 100 mm diameter entrance admittance, subsonic (200m/sec mean velocity) missile, the approach of which is to be simulated at 1600m to 40m from a target. If the available lens carrying stages are bounded by a maximum speed of 1000 mm/sec on the optical bench, then from equation (1) the velocity indicator of the zoom designed should not exceed 200 mm at the critical moment of the missile's nearest approach.

A zoom to fit this need is shown as a first order general solution in Figure 1 (a) through (c), and then as a fully developed implementation for the Mid IR spectral region (3 to 5 μ), in Figure 2 (a) through (c), with the air spaces and indicators versus EFL in table (Figure) 3.

In all figures, surfaces and groups are numbered from the UUT side toward the projected Thermoscene² focal plane, and show only the zoom proper with or without the condenser element that interfaces the radiation source (blackbody) present on each focal plane. In the first-order diagrams of Figure 1, surface #1 stands for an intermediate pupil, surfaces #2, and #3 represent two stationary groups (real surfaces 28 to 31 and then 32 to 35 on the fully developed zoom of Figure 2), surfaces #4 and #5 are the two movable groups (real surfaces 36 to 39 and 40 to 45), surface #6 is a last stationary group (real surface 46 to 49), surface #7 is the Thermoscene focal plane, surface #8 the condenser element (not shown on the fully developed solution), and surface #9 represent the blackbody opening. In the table (Figure 3) the changeable principal planes air-spacing and the indicators of the two moving groups are shown as a function of the EFL for each entry, at fifty intermediate positions are shown as function of the EFL and the indicators of the two moving groups at each entry.

Spanning only a range 1:3.5 EFLs, the zoom should be triply cascaded, as shown in fig 4, to cover the entire approach range of 1:40 of simulated flight. From the table (Figure 3), the velocity indicator of the faster group at the 200 mm EFL end is 146.5 mm meaning that its absolute value there is 735 mm/sec, safely below the maximum permissible. Assuming the missile acceleration to be null at this moment, then, according to equation (5), the fast stage acceleration is 4550 mm/sec², somewhat less than 0.5g. To brake this stage within the 30 mm air space available to it at this end a deceleration of 0.9g must be applied - a quite conservative regime.

A point to be noted is that the availability of a braking space in the solution shown, sufficient for stopping safely the second moving group, is not apparent in the first order layout of Fig 1. As shown there, the principal planes of this group and the stationary one following it are almost in contact at the short EFL end of the zoom. Higher order design, however, succeeded in this case to make the actual air spacing between those groups large enough to provide a safe braking relief, though the appropriate principal plane are still in contact, of course, at this EFL.

4. SIMULATION SEQUENCE

Figure 4 shows the actual implementation of part of the optics of the example described in the previous Section (the condenser elements between the sources and the Thermoscenes are not shown). The concept is based on the combination of two identical optical channels (1 and 2), which are partly physically separated, and partly common. Figure 4 shows, starting from the exit pupil plane no. 3 where the UUT entrance admittance's real image is located, the first group common to both channels, then a transition mirror at 45 degrees, and then the two physically separated trains of lenses. Planes 1 and 2 are the intermediate focal planes where the Thermoscenes are located. The transition mirror is capable of moving in and out of the optical beam (perpendicular to the plane of the paper) very fast, so that only one channel is active at one time. The fast transition is needed to avoid discontinuous spurious events during the scenario.

The simulation sequence for the whole approach scenario is covered by four stages in which the two optical channels are alternatively active. At first, channel 1 is active (transition mirror in the optical beam), the focal length is longest (to simulate the longest distance of 1600 meters), and the first Thermoscene carries the image of the scene with the largest amount of background and the smallest magnification: the lenses start to move with the EFL decreasing from 700 to 200 mm (to simulate approach to 450 meters), at which time the transition mirror moves out of the beam, letting channel 2 to be active. In the intermediate focal plane of channel 2 there is a previously mounted Thermoscene with the identical image as the first one, except that it is magnified by a factor 3.5. The lens movement is then performed in channel 2, simulating the approach from 450 to 130 meters (again a factor 3.5), while a third appropriately magnified Thermoscene is brought to the intermediate focal plane of channel 1 by a rotary or translatory stage to prepare for the next stage of simulation. At this point the transition mirror moves into the beam, activating channel 1, and the lens movement repeated, while a fourth Thermoscene is similarly prepared in channel 2. In the fourth stage the same process is repeated for the last time.

5. CONCLUSION

We have dealt in this paper with the special characteristics that must be endowed to a dynamic zoom to make it useful as a faithful projector in real time simulation of evolving scenes. We have shown that translation lens stage velocity and acceleration as well as braking relief at the short EFL end set a limit to true simulation in high performance dynamic zooms used for missile tests. We have applied these new principles to an approach scenario over 1:40 range ratio of a 10 degree FOV, 100 mm admittance opening, subsonic missile seeker head in the Mid IR region (3-5 μ).

6. ACKNOWLEDGEMENT

The authors wish to acknowledge the continuous interest shown by Dr. Dario Cabib, CI Systems' Technical Director, in this work, and his actual help during some of its phases.

7. REFERENCES

1. E. Ben-David and Dario Cabib, "IR simulation of missile closing on a moving textured object with a textured background and EO countermeasure", *SPIE Proceedings*, Vol. 1687, pp. 509-521, September 1992.
2. Dario Cabib, Joshua Eliason, Bob Hermes, Emanuel Ben-David, Shai Ghilai and Ronni Bracha, "Accurate infrared scene simulation by means of microlithographically deposited substrate", *SPIE Proceedings*, Vol. 1762, pp. 376-384, January 1993.

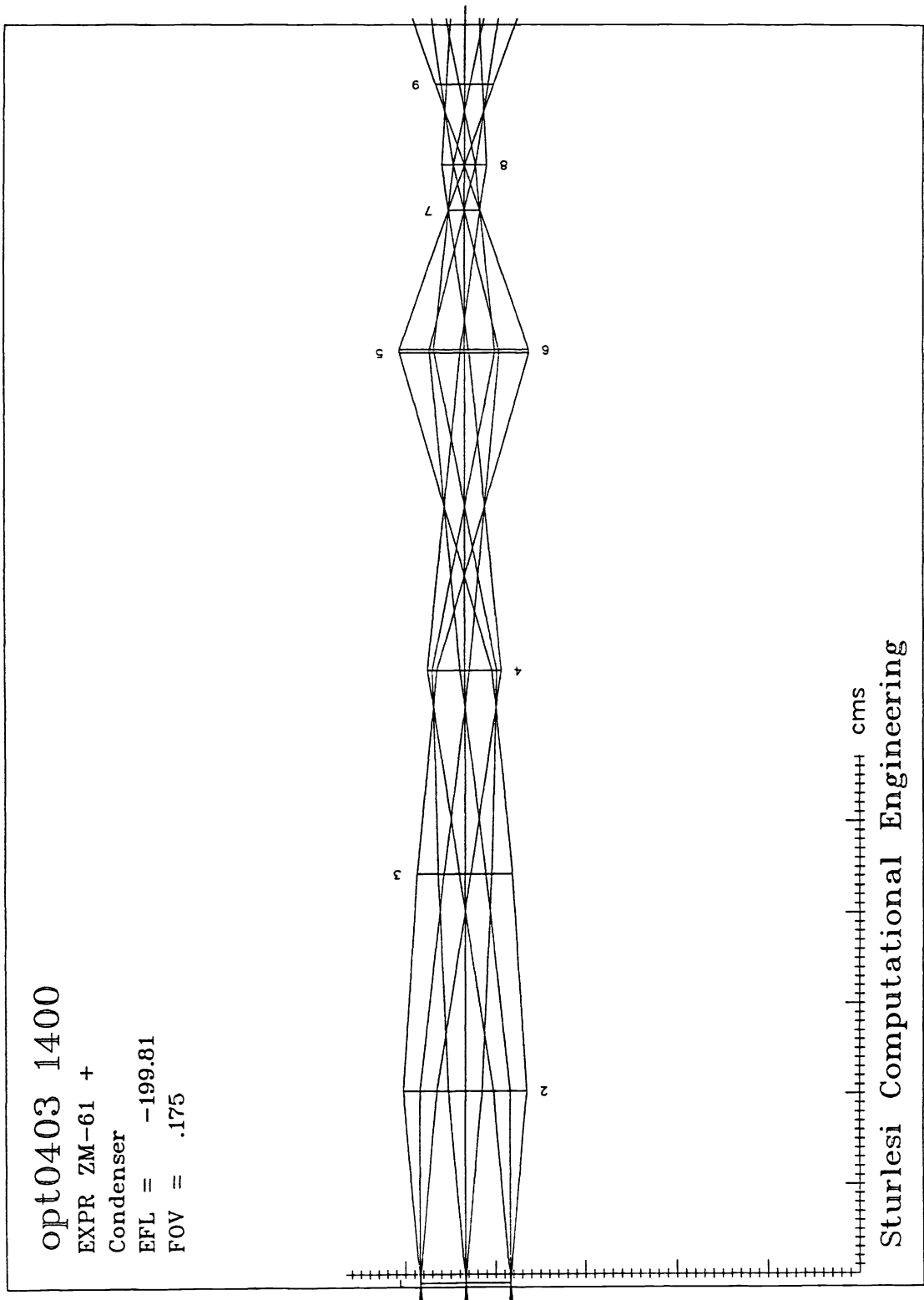


Figure 1 (a). First order general solution of an example of dynamic zoom presenting a 10 degrees Field of View scene to a missile seeker head, showing the principal planes positions of the lens groups. EFL = 199.81 mm.

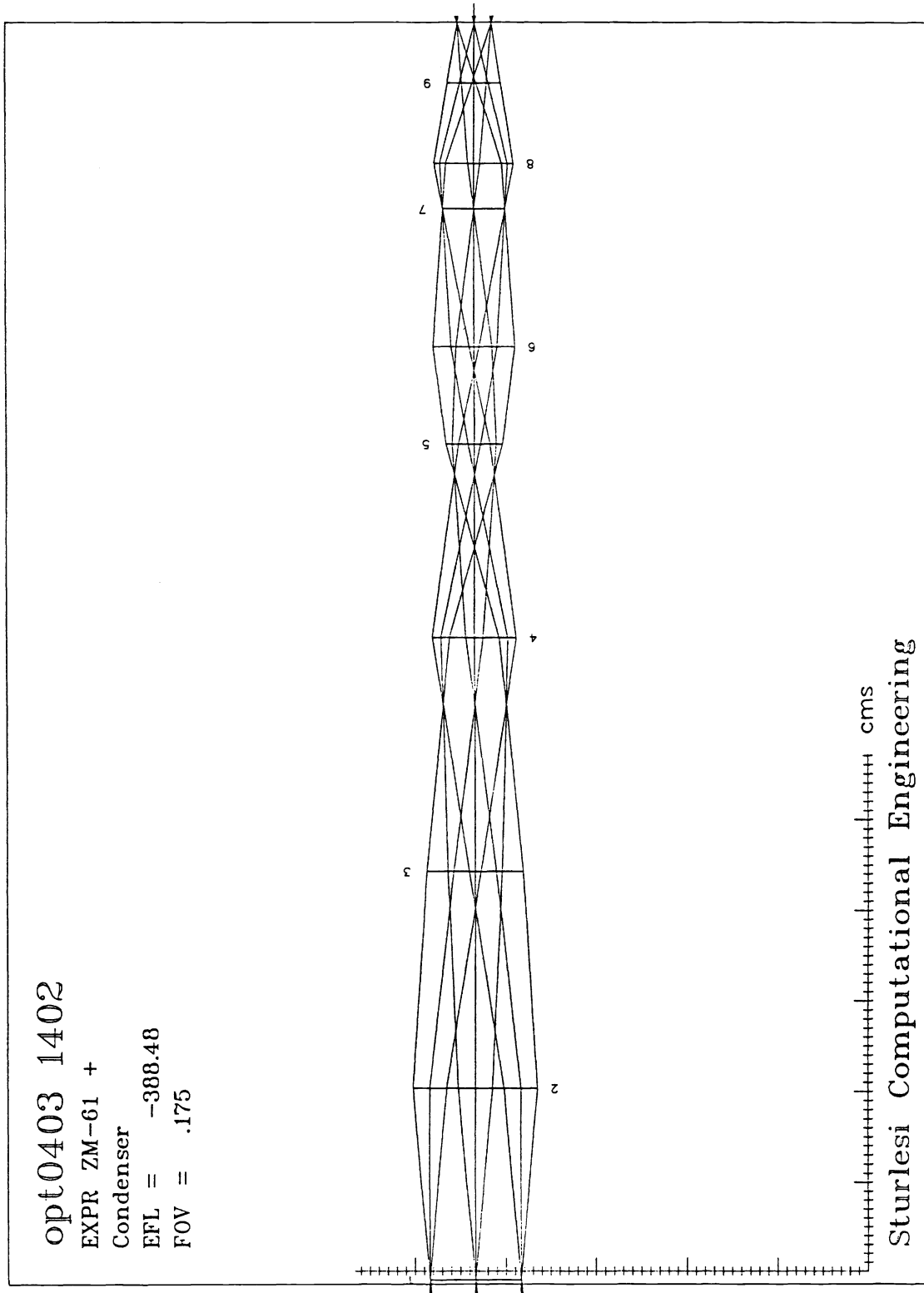


Figure 1 (b). First order general solution of an example of dynamic zoom presenting a 10 degrees Field of View scene to a missile seeker head, showing the principal planes positions of the lens groups. EFL= 388.48 mm.

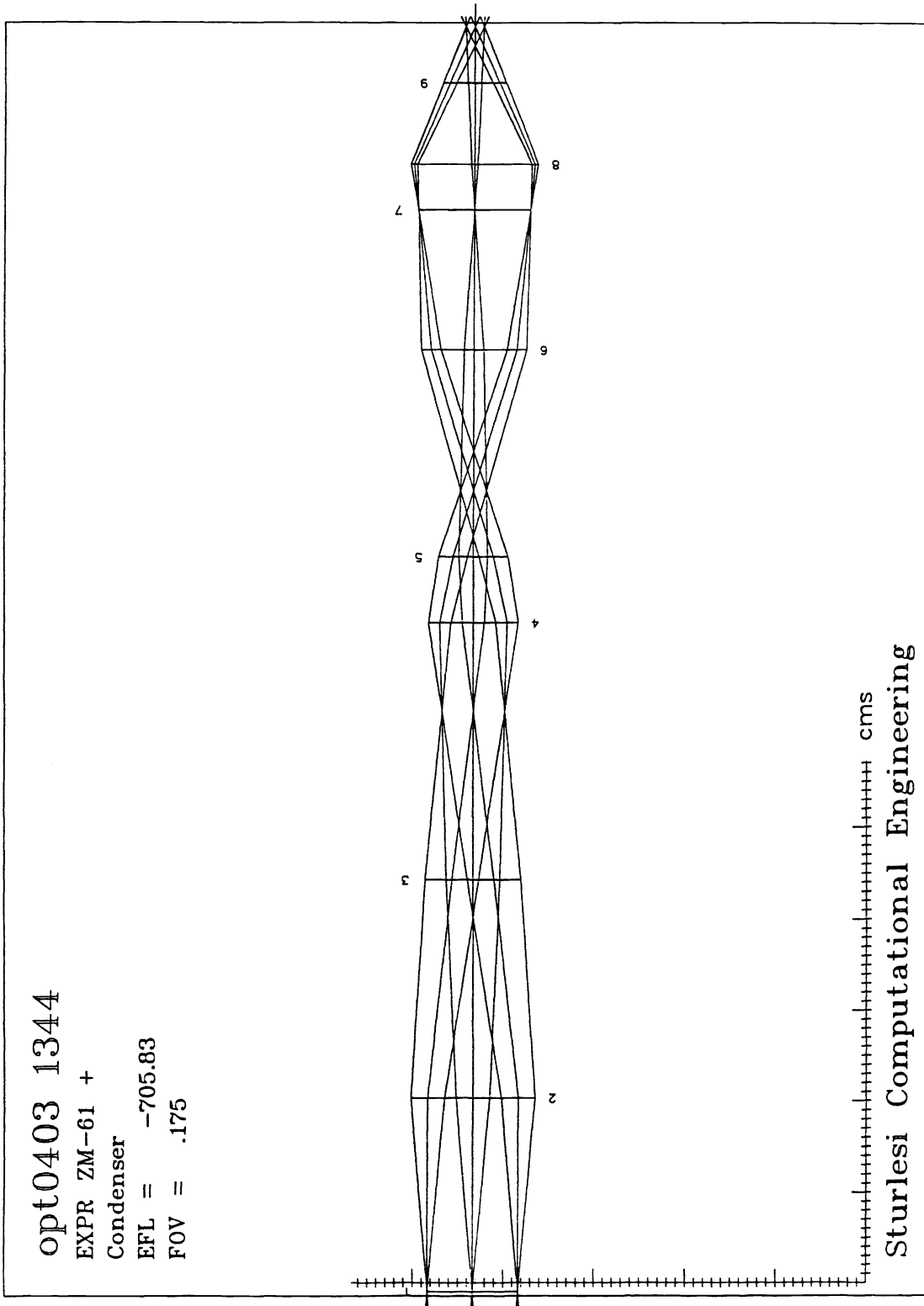


Figure 1 (c). First order general solution of an example of dynamic zoom presenting a 10 degrees Field of View scene to a missile seeker head, showing the principal planes positions of the lens groups. EFL= 705.83 mm.

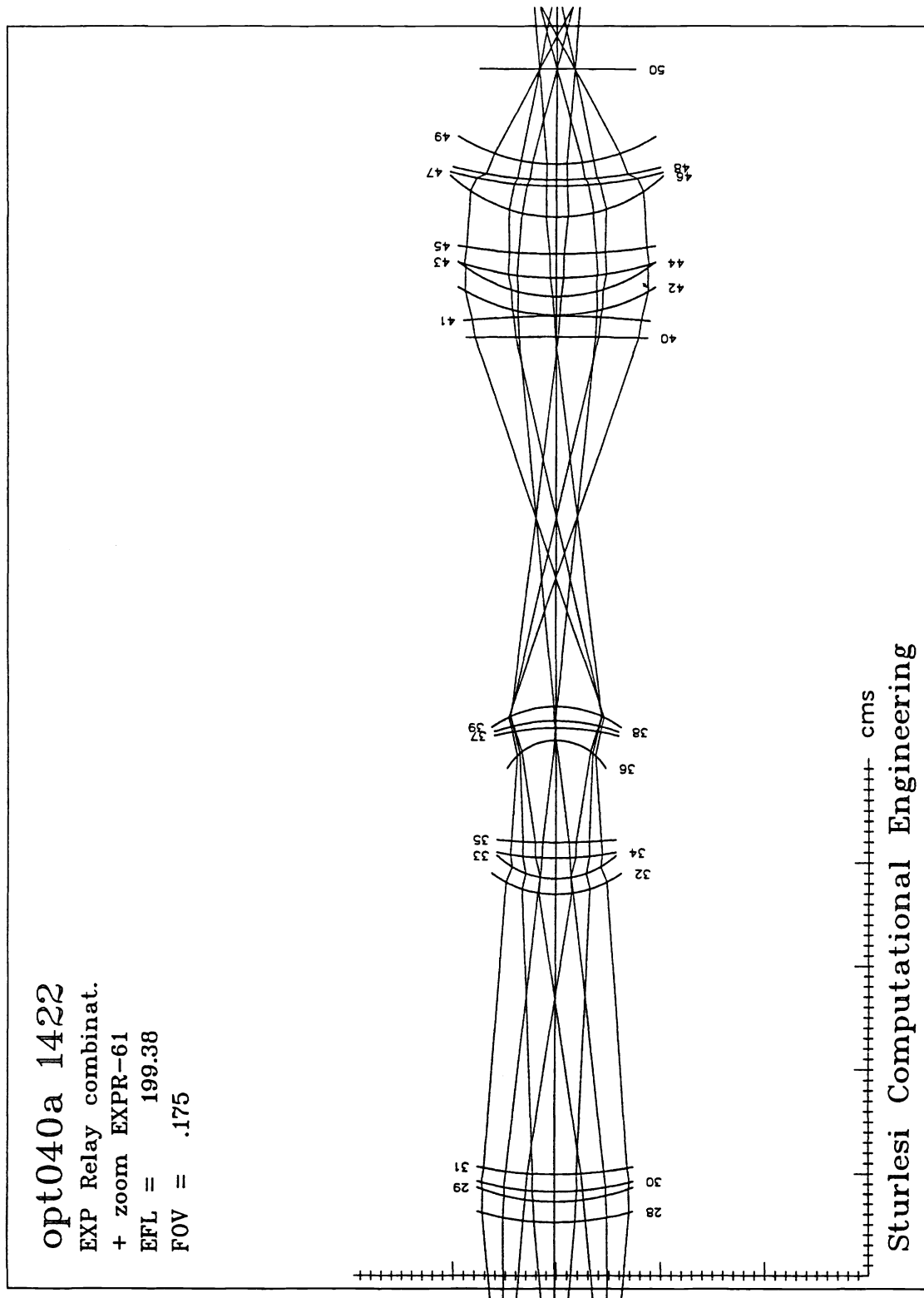


Figure 2 (a). Optical surfaces positions of the dynamic zoom system of Figure 1. (a) EFL = 199.38 mm, fully developed for the Mid IR wavelength range.

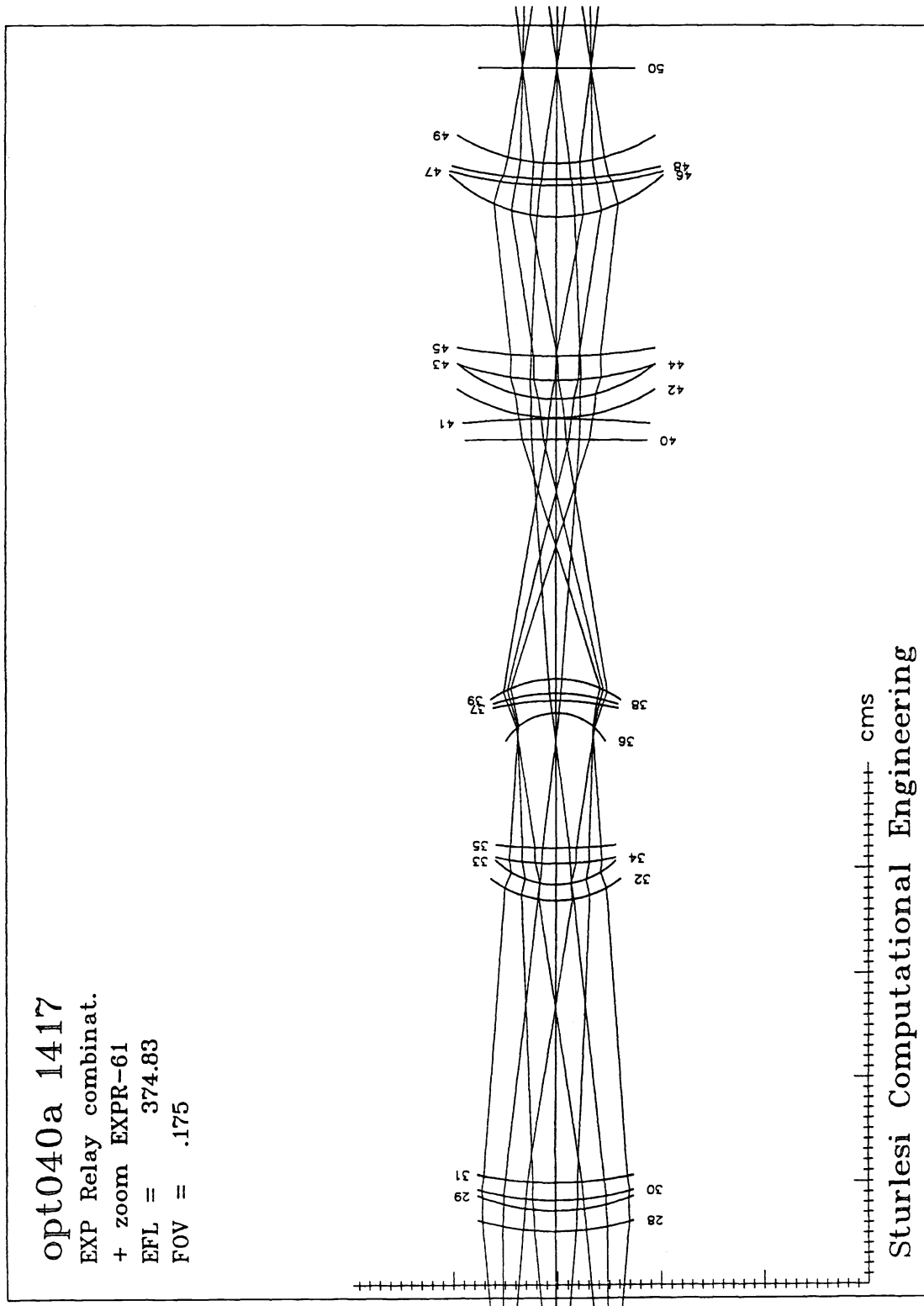


Figure 2 (b). Optical surfaces positions of the dynamic zoom system of Figure 1. (b) EFL = 374.83 mm, fully developed for the Mid IR wavelength range.

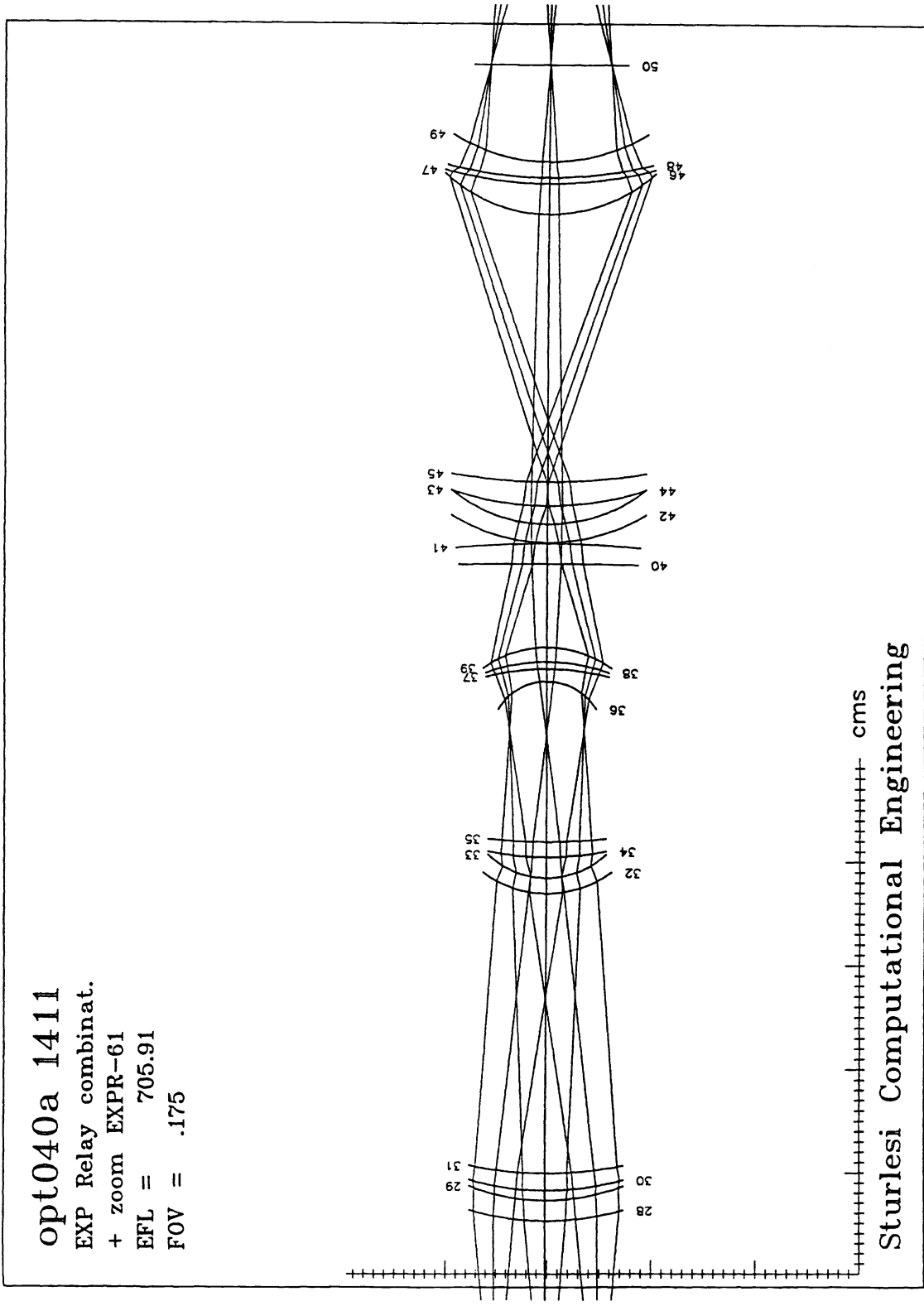


Figure 2 (c). Optical surfaces positions of the dynamic zoom system of Figure 1. (c) EFL =705.91 mm, fully developed for the Mid IR wavelength range.

TABLE I (zoom EXPR-61)
 (all numerical values shown have linear dimension and are given in mm)
 from 200. to 700. EFL (1:3.5)

	Air Spaces			EFL	velocity indicator $f \cdot dx/df$		acceleration indicator $f^2 \cdot d^2x/df^2$		
	II-III	III-IV	IV-V		GIII	GIV	GIII	GIV	
1	224.225	352.500	3.555	-199.794	52.25	-146.51	-21.73	181.72	1
2	225.741	346.786	7.753	-205.620	52.98	-145.73	-33.22	164.19	2
3	227.271	341.072	11.936	-211.614	53.43	-145.39	-42.18	150.32	3
4	228.810	335.358	16.112	-217.777	53.66	-145.40	-49.08	139.41	4
5	230.350	329.644	20.286	-224.110	53.73	-145.69	-54.41	130.75	5
6	231.887	323.930	24.463	-230.614	53.66	-146.21	-58.53	123.83	6
7	233.416	318.216	28.647	-237.289	53.48	-146.92	-61.72	118.27	7
8	234.935	312.502	32.843	-244.138	53.22	-147.80	-64.17	113.78	8
9	236.440	306.788	37.051	-251.161	52.89	-148.82	-66.04	110.16	9
10	237.930	301.074	41.275	-258.360	52.51	-149.96	-67.43	107.24	10
11	239.403	295.360	45.517	-265.737	52.08	-151.20	-68.45	104.89	11
12	240.857	289.646	49.777	-273.292	51.62	-152.53	-69.16	103.01	12
13	242.292	283.932	54.056	-281.028	51.13	-153.94	-69.63	101.52	13
14	243.706	278.218	58.356	-288.945	50.62	-155.42	-69.88	100.37	14
15	245.098	272.504	62.677	-297.046	50.09	-156.96	-69.97	99.49	15
16	246.470	266.790	67.020	-305.331	49.55	-158.56	-69.91	98.84	16
17	247.819	261.076	71.385	-313.803	49.00	-160.22	-69.74	98.40	17
18	249.145	255.362	75.772	-322.463	48.45	-161.92	-69.47	98.13	18
19	250.450	249.648	80.182	-331.312	47.89	-163.66	-69.13	98.01	19
20	251.732	243.934	84.614	-340.352	47.32	-165.44	-68.72	98.02	20
21	252.991	238.220	89.069	-349.583	46.76	-167.26	-68.25	98.14	21
22	254.228	232.506	93.546	-359.008	46.20	-169.11	-67.74	98.36	22
23	255.443	226.792	98.045	-368.628	45.64	-171.00	-67.19	98.67	23
24	256.635	221.078	102.567	-378.443	45.09	-172.91	-66.61	99.06	24
25	257.805	215.364	107.110	-388.456	44.53	-174.86	-66.01	99.51	25
26	258.954	209.650	111.676	-398.667	43.99	-176.83	-65.39	100.03	26
27	260.082	203.936	116.262	-409.077	43.45	-178.82	-64.75	100.60	27
28	261.188	198.222	120.870	-419.688	42.91	-180.84	-64.10	101.22	28
29	262.273	192.508	125.499	-430.501	42.38	-182.88	-63.45	101.88	29
30	263.337	186.794	130.149	-441.517	41.86	-184.94	-62.79	102.58	30
31	264.382	181.080	134.818	-452.737	41.34	-187.02	-62.12	103.32	31
32	265.406	175.366	139.508	-464.161	40.83	-189.12	-61.45	104.09	32
33	266.410	169.652	144.217	-475.792	40.33	-191.24	-60.78	104.90	33
34	267.396	163.938	148.946	-487.629	39.84	-193.38	-60.12	105.73	34
35	268.362	158.224	153.694	-499.673	39.35	-195.53	-59.45	106.58	35
36	269.310	152.510	158.460	-511.927	38.87	-197.70	-58.79	107.46	36
37	270.239	146.796	163.244	-524.389	38.40	-199.89	-58.14	108.36	37
38	271.151	141.082	168.047	-537.062	37.94	-202.09	-57.49	109.28	38
39	272.045	135.368	172.867	-549.946	37.48	-204.31	-56.84	110.21	39
40	272.922	129.654	177.704	-563.041	37.03	-206.54	-56.21	111.17	40
41	273.782	123.940	182.558	-576.349	36.59	-208.78	-55.58	112.14	41
42	274.626	118.226	187.428	-589.871	36.15	-211.04	-54.95	113.12	42
43	275.453	112.512	192.314	-603.606	35.73	-213.31	-54.34	114.12	43
44	276.265	106.798	197.217	-617.555	35.31	-215.59	-53.73	115.14	44
45	277.061	101.084	202.135	-631.720	34.89	-217.88	-53.13	116.16	45
46	277.842	95.370	207.068	-646.100	34.49	-220.19	-52.53	117.20	46
47	278.608	89.656	212.015	-660.697	34.09	-222.50	-51.95	118.25	47
48	279.360	83.942	216.978	-675.511	33.70	-224.83	-51.37	119.31	48
49	280.098	78.228	221.954	-690.542	33.31	-227.17	-50.81	120.37	49
50	280.821	72.514	226.945	-705.791	32.93	-229.52	-50.25	121.45	50

Figure 3. Air spaces between the lens groups, velocity and acceleration indicators versus EFL for the dynamic zoom of Figure 1. (a) distance II-III, (b) distance III-IV, (c) distance IV-V, (d) velocity indicators for III and IV, (e) acceleration indicators for III and IV.

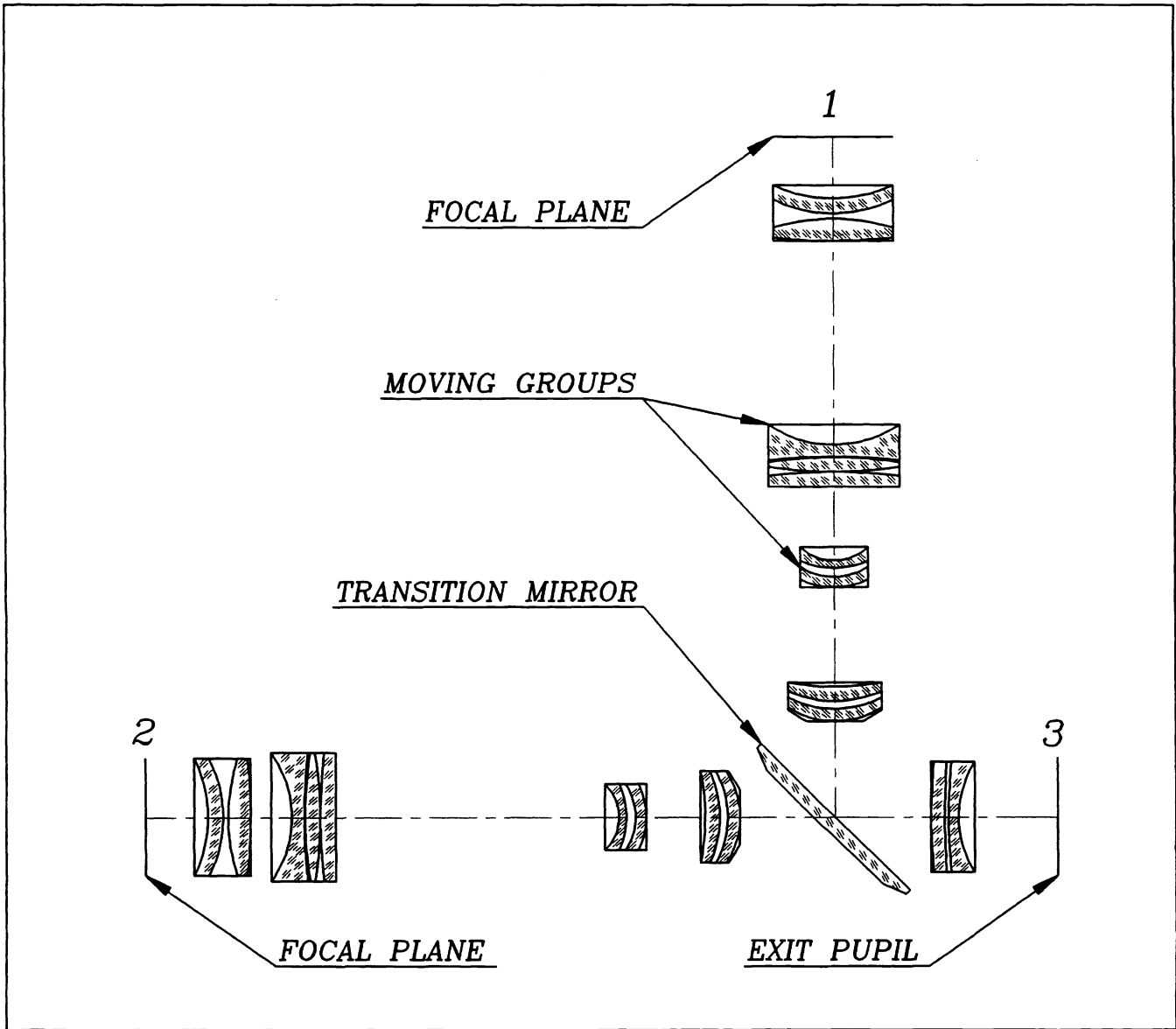


Figure 4. Optical layout of a triply cascaded 1:40 Mid IR zoom. 1 and 2 are the focal planes where the Thermoscenes are located, and 3 is the exit pupil plane where the missile seeker entrance pupil is located. The two moving groups in each channel are the surfaces 36 to 39 and 40 to 45 of Figure 2.